

Dependence of the structure, optical phonon modes and dielectric properties on pressure in wurtzite GaN and AlN

H. WANG^{a,b*}, Y. XIE^a, Y. LI^{a,c}, N. ZHANG^a

^aDepartment of Physics and Electronic Information Engineering, Xiangnan University, Chenzhou 423000, China

^bSchool of physics and electronics, Central South University, Changsha 410083, China

^cCollege of physical science and technology, Huazhong Normal University, Wuhan 430079, China

The density functional perturbation theory (DFPT) is employed to study the structure, optical phonon modes and dielectric properties for wurtzite GaN and AlN under hydrostatic pressure. In order to calculate accurately the Born effective charges and high frequency dielectric tensors, we utilize two sum rules to monitor this calculation. The calculated optical phonon frequencies and longitudinal-transverse splitting show an increasing with pressure, whereas the Born effective charges, and high frequency dielectric tensors are found to decrease with pressure. In particular, we analysed the reason for discrepancy between this calculation and previous experimental determination of pressure dependence of the LO-TO splitting in AlN. The different pressure behavior of the structural and lattice-dynamical properties of GaN and AlN is discussed in terms of the strengths of the covalent bonds and crystal anisotropy. Our results regarding dielectric Grüneisen parameter are predictions and may serve as a reference.

(Received July 28, 2014; accepted September 9, 2015)

Keywords: GaN AlN; Lattice dynamics; Dielectric; Pressure

1. Introduction

The group-III nitrides GaN and AlN are currently being actively investigated in view of their promising potential for short-wavelength electroluminescence devices and high-temperature, high-power, and high-frequency electronics [1-5]. An important motivation for high-pressure investigations stems from the fact that group-III-nitride layers are commonly subjected to large built-in strain since they are often grown on different substrates having considerable lattice mismatch.

The understanding the effect of pressure on the vibrational properties is quite important. Its knowledge allows one to correlate macroscopic thermodynamic parameters with properties on the atomic scale. The neutron scattering, electron energy loss spectroscopy, IR absorption, Raman spectroscopy, diamond anvil cell etc. experimentally have been used to study phonons and related properties. Perlin et al.[6] and Kuball et al.[7] performed the high-pressure Raman studies for AlN, estimating the pressure coefficients of Raman-active modes. They reported that under pressure the LO-TO (E_1) splitting slightly decreases and the LO-TO (A_1) splitting increases. Afterwards, Goñi et al. [8] compared the pressure dependence of the Raman-active modes in GaN and AlN with ab initio calculations and found a small but

increasing LO-TO (E_1) splitting under pressure. However, a decrease of the LO-TO splitting for both A_1 and E_1 modes in AlN was estimated in recent Raman measurements of Yakovenko et al. [9] and Francisco et al. [10]. Meanwhile, Francisco et al. studied the optical phonon modes and pressure dependences of AlN by means of ab initio lattice dynamical calculations, but being a increase of the LO-TO splitting for both A_1 and E_1 modes. Perlin et al. [11] compared pressure dependence of the A_1 (TO), A_1 (LO) phonon modes and effective transverse charge of wurtzite GaN by Raman scattering and means of tight-binding formalism. In contrast with the extensive range of experimental studies on the pressure effect on the phonon dispersion of semiconductors, theoretical works on the topic are relatively sparse. The pressure dependence of the LO-TO splitting in GaN and AlN is an issue of controversy. In a polar lattice, the splitting of the optical phonon modes is determined by two parameters, Born effective charge of the lattice ions and the screening of the Coulomb interaction, which depends on the electronic part of the dielectric constant in the phonon frequency regime.

In this work, we study the pressure effect on phonon and relevant properties for GaN up to 50 GPa and AlN up to 20 GPa by DFPT computations. Because experimental measurements show that GaN and AlN

transform from the wurzite to the rocksalt phase under high pressure. Such a phase transition has been reported to start at 55.1 *GPa* by P. E. Van Camp et al. [12] and 52.2 *GPa* by M. Ueno et al. [13] for GaN. For AlN, corresponding to a transition pressure of 22.0 *GPa* by Ueno et al. [14] and 20.0 *GPa* by Uehara et al. [15]. Firstly, we calculate and analyse the evolution with pressure of the unit cell shape (i.e., *c/a* ratio) and unit cell geometry (i.e., internal parameter *u*) of GaN and AlN. In the following section, study pressure dependence of zone-center optical phonon modes and the LO–TO splitting of both the A_1 and E_1 modes. Next, calculate and discuss the pressure dependence of Born effective charge tensors Z^* and the high frequency dielectric tensor ϵ^∞ . Finally, predict dielectric Grüneisen parameter γ .

2. Theory and computational details

2.1 Theory

The interatomic force constants (IFC's) describing the atomic interactions in a crystalline solid are defined in real space as [16]

$$C_{k\alpha,k'\beta}(a,b) = \frac{\partial^2 E}{\partial \tau_{k\alpha}^a \partial \tau_{k'\beta}^b}, \quad (1)$$

$$\epsilon_{\alpha\beta}(\omega) = \epsilon_{\alpha\beta}^\infty + \frac{4\pi}{\Omega_0} \sum_{kk'} \sum_{\alpha'\beta''} Z_{k,\alpha\alpha'}^* [\tilde{C}(q=0) - M \omega^2]_{k\alpha',k'\beta'}^{-1} Z_{k',\beta\beta''}^*, \quad (3)$$

Where $\epsilon_{\alpha\beta}^\infty = \delta_{\alpha\beta} - \frac{4\pi}{\Omega_0} 2 E_{el}^{\epsilon_\alpha \epsilon_\beta}$ is electronic

contribution to the dielectric constant; $E_{el}^{\epsilon_\alpha \epsilon_\beta}$ is the second derivative of the total electronic energy with respect to a perturbing electric field along directions α and β ; Ω_0 and M are the unit cell volume and mass; To other variables, see Ref. 16.

The Born effective charge is defined as the variation of the force on a given atom under the application of an electric field

$$Z_{k,\beta\alpha}^* = \Omega_0 \frac{\partial P_{mac,\beta}}{\partial \tau_{k\alpha}}(q=0) = \frac{\partial F_{k,\alpha}}{\partial \epsilon_\beta}, \quad (4)$$

where $P_{mac,\beta}$ is the macroscopic electric polarization induced by the screened electric field. In order to calculate accurately the Born effective charges and

Here, $\tau_{k\alpha}^a$ is the displacement vector of the *k*th atom in the *a*th primitive unit cell (with translation vector \vec{R}_a) along the α axis. E is the Born-Oppenheimer (BO) total energy surface of the system (electrons plus clamped ions).

The vibration frequencies ($\omega_{j,\vec{q}}$) and polarization vectors [$\vec{e}_k(\vec{q}|j)$] of the phonon modes with wave vector \vec{q} are determined by solving the eigenvalue matrix equation

$$\sum_{k\beta} \tilde{D}_{k\alpha,k'\beta}(\vec{q}) e_{k'\beta}(\vec{q}|j) = \omega_{j,\vec{q}}^2 e_{k,\alpha}(\vec{q}|j) \quad (2)$$

Where $\tilde{D}_{k\alpha,k'\beta}(\vec{q})$ is the dynamical matrix, which is related to the Fourier transform of the IFC's.

The dielectric constant mainly is influenced by two factors which are the electron and phonon,

dielectric constant, we utilize two sum rules to monitor calculation. The first is the acoustic-sum rule: the dynamical matrix at the zone center should admit the homogenous translations of the solid

$$\sum_{k'} \tilde{C}_{k\alpha,k'\beta}(q=0) = 0. \quad (5)$$

The second sum rule guarantees that the charge neutrality is also fulfilled at the level of the Born effective charges. For every direction α and β , one must have

$$\sum_k Z_{k,\alpha\beta}^* = 0. \quad (6)$$

By the above sum rules, we can monitor whether the calculation is well converged with respect to numerical parameters, like the number of plane waves, the sampling of BZ, and the number of points of the

exchange-correlation grid.

2.2 Computational details

We use a first-principles pseudopotential method based on the density functional perturbation theory with wave function represented in a plane-wave basis set. This work is performed employing the ABINIT package [17]. A review of the method (and of the algorithm used for the convergence of electronic density and atomic positions) can be found in Ref. 18. The effect of the approximation to the exchange-correlation (XC) energy is considered. The pseudopotential for Ga, Al and N atoms are generated according to scheme of Troullier and

Martin [19]. Brillouin-zone integrations were performed using $12 \times 12 \times 8$ k-point mesh, and phonon frequencies were computed on a $6 \times 6 \times 4$ q-point mesh. Plane-wave basis sets with a cutoff of 40 Hartree were used. These calculating parameters are chosen to guarantee the total energy error in 0.1 mHartree.

3. Results and discussion

In Fig. 1, we show the evolution with pressure of the unit cell shape (i.e., c/a ratio) and unit cell geometry (i.e., internal parameter u) of the wurtzite structure GaN and AlN.

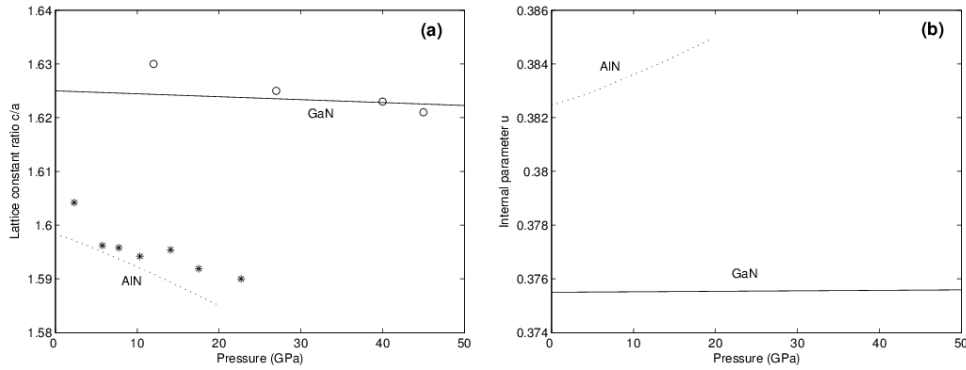


Fig. 1. Structural parameters of wurtzite GaN and AlN under hydrostatic pressure. Asterisk and open circles are experimental results from Ref. 14 for GaN and Ref. 13 for AlN.

The calculations were performed in two steps. In the first step, we calculate the total energy of the bulk wurtzite crystal as a function of the unit cell volume. Then, using the definition of pressure, $P = -\partial E_{tot} / \partial V$, one can find the unit cell volume corresponding to the certain value of the external pressure P . In this step, for a given unit cell volume, c/a and u are optimized. As can be seen from these figs. 1(a) and 1(b), one can correlate the magnitude of changes in c/a and u under the hydrostatic pressure with deviations of the nitride structures from “ideal” wurtzite. The weaker dependences of c/a and u on the hydrostatic pressure are obtained for GaN, which possesses the smaller deviation of c/a from the ideal value 1.633. We find linear pressure coefficients of

$$\left(\frac{\partial c}{\partial p}\right)_{p=0} = -5.45 \times 10^{-5} \quad \text{and} \quad \left(\frac{\partial u}{\partial p}\right)_{p=0} = 1.81 \times 10^{-6}$$

for GaN. In the case of AlN, the situation is completely different. The values c/a (u) are remarkably smaller (larger) than the ideal values and decrease (increase) with rising hydrostatic pressure, with a slope of

$$\left(\frac{\partial c}{\partial p}\right)_{p=0} = -6.86 \times 10^{-4} \quad \text{and} \quad \left(\frac{\partial u}{\partial p}\right)_{p=0} = 1.27 \times 10^{-4}.$$

Our results for c/a are in reasonable agreement with experimental studies of the lattice constants under pressure [14,13].

For most stable wurtzite-type structures c/a ratio and the u parameter are strongly correlated; If c/a decreases, then u increases in such a way that the inequivalent bond lengths $R^{(l)}$ (along the c direction with bond length

$R^{(1)} = uc$) and $R^{(2)}$ are nearly equal, however, the tetrahedral angles are distorted. The bond lengths $R^{(1)}$ and $R^{(2)}$ (in the hexagonal plane and is threefold degenerate with bond length $R^{(2)} = \sqrt{1/3 + (1/2 - u)^2 (c/a)^2}$) would be equal if $u = a^2 / (3c^2) + 1/4$. The

so-estimated value of the internal parameter u of GaN (0.3754) nearly agrees with the calculated one (0.3745). In the case of AlN there is, however, a larger deviation between the estimated value (0.3784) and the calculated one (0.3803). This finding can be attributed to the stronger covalent bonding of AlN, which preserves the ideal tetrahedral bond angles.

Table 1. Fitting parameters used for the pressure dependence of the phonon frequencies in GaN and AlN. For comparison theoretical and experimental results in other literatures are also shown. Units are (cm⁻¹/GPa)

		$A_1(TO)$	$E_1(TO)$	$A_1(LO)$	$E_1(LO)$
GaN	Calc. ^a	3.10	3.08	3.42	3.432
	Expt. ^b	3.9	3.94	4.4	
	Expt. ^c	3.55		3.2	
	Calc. ^d	3.1	3.3	3.5	3.6
AlN	Calc. ^a	3.05	2.96	3.48	3.50
	Expt. ^e	4.08	5.07	4.00	
	Expt. ^f	4.35	5.33	3.70	4.77
	Expt. ^g	4.05	4.52	4.00	3.60
	Calc. ^h	3.00	3.80	3.50	4.00

^a This work, ^b Ref. 8, ^c Ref. 11, ^d Ref. 8, ^e Ref. 7, ^f Ref. 10, ^g Ref. 9, ^h Ref. 8

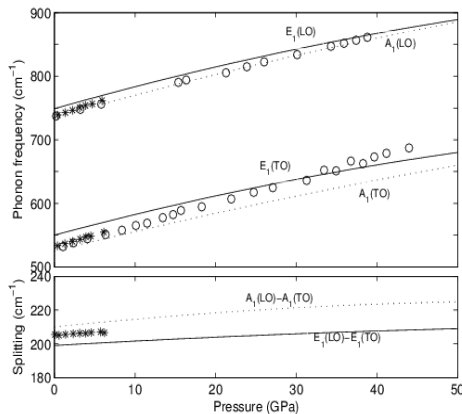


Fig. 2. The zone-center optical frequencies for the wurtzite GaN as functions of pressure (upper panel). Pressure dependence of the LO-TO splitting for both the A_1 and E_1 modes in GaN (lower panel). Open circles and asterisk are taken from experimental results for A_1 from Ref. 11 and Ref. 8 for GaN respectively.

The pressure dependence of zone-center optical

phonon modes and the LO-TO splitting of both the A_1 and E_1 modes are plotted in Fig. 2 (GaN) and Fig. 3 (AlN). Table 1 summarizes fitting pressure coefficients of the A_1 and E_1 . In general, The agreement between our calculated values at zero pressure and other theoretical values [8] is reasonably good. The calculated frequencies are slightly above other experimental data, which is likely due to underestimation of the lattice parameters as is usual in DFT-LDA calculations. Also, the calculated pressure coefficients are typically smaller than other experimental values. Also interesting is the difference between the pressure dependence of the LO-TO splittings in AlN. According to our calculations both the LO-TO splitting of both the A_1 and E_1 modes are almost constant or even increase slightly with increasing pressure. an increase of the LO-TO splitting for the A_1 mode was found Manjón et al.[20] and Goñi et al. [8] and attributed to the decrease of the refractive index with pressure in AlN as suggested by ab initio calculations [21]. The experimental discrepancies could be due to differences in sample preparation and pressure environment that may affect the pressure response of the Raman modes in AlN [9]. Additionally, the weak intensity of the TO and LO modes

reported by Kuball et al. [7] might have resulted in an inaccurate determination of the pressure coefficients and LO–TO splittings.

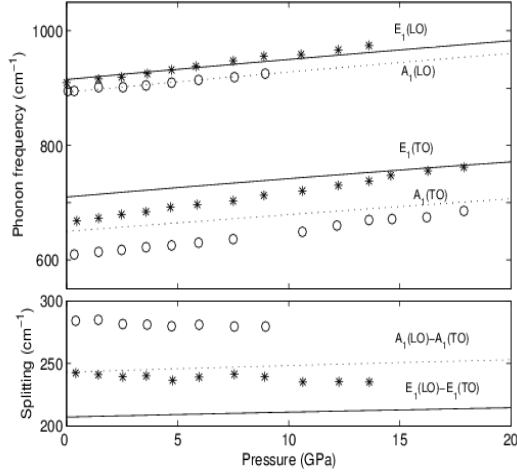


Fig. 3. The zone-center optical frequencies for the wurtzite AlN as functions of pressure (upper panel). Pressure dependence of the LO–TO splitting for both the A_1 and E_1 modes in GaN (lower panel). Open circles and asterisk are taken from experimental results for A_1 and E_1 from Ref. 10 for AlN respectively.

Taking the angular dispersion of the TO modes, $[\omega_{TO}(E_1) - \omega_{TO}(A_1)] / \omega_{TO}(E_1)$ as a measure of the crystal anisotropy, we find 0.081 for AlN and 0.045 for GaN. AlN is thus more anisotropic than GaN, which is coincident with former discuss.

The LO–TO splitting is a function of Born effective charges Z^* and infrared dielectric constant ϵ_∞ . For modes of the same symmetry with atomic displacements along direction α ($\alpha=x, z$) one finds [22]

$$\omega_{LO}^2(\alpha) - \omega_{TO}^2(\alpha) = \frac{2e^2(Z^*)_{\alpha\alpha}^2}{\epsilon_0(\epsilon_\infty)_{\alpha\alpha}V\mu}, \quad (7)$$

where ϵ_0 is the vacuum permittivity, μ is the reduced mass of an anion-cation pair, V is the available volume per pair, and ω is the angular mode frequency given in hertz. The change of the Born effective charge under compression can be determined from the measured frequencies of the optical phonons using Eq. (7). Born effective charge tensors determine, with the high frequency dielectric tensor ϵ_∞ , the strength of Coulomb

interaction which is responsible for the splitting between the transverse (TO) and the longitudinal (LO) optical modes. It is a measure of the change in electronic polarization due to ionic displacements. For atom k , $Z_{k,\beta\alpha}^*$ quantifies to linear order the polarization per unit cell, created along the direction β when the atoms of sublattice k are displaced along the direction α , under the condition of zero electric field.

Although there are four atoms in the unit cell of the wurtzite structure the nonsymmorphic space group C_{6v}^4 with a screw along the c axis enforces that only two of them are independent. Furthermore, because of the acoustic sum rule:

$$\sum_k Z_{k,\alpha\beta}^* = 0,$$

Only two independent components $Z_{||}^*$ and Z_{\perp}^* of Born effective charge tensor are existent. Contrary to the effective charges, the form of the dielectric tensor is determined by the symmetry of the crystal and is expected to be diagonal for the wurtzite structure. The dielectric tensors ϵ_∞ should have two independent components $\epsilon_\infty^{||}$ and ϵ_∞^{\perp} along and perpendicular to the c axis, respectively.

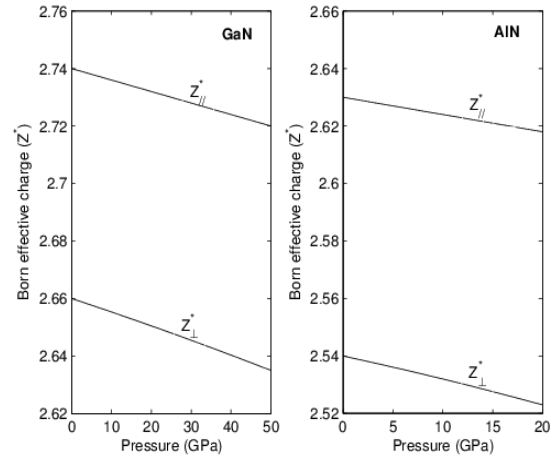


Fig. 4. Born effective charge versus pressure for wurtzite GaN and AlN

The calculated Born effective charge tensors at zero pressure agree well with the experimental data obtained from first-order Raman-scattering experiments.[23, 24] To the best of our knowledge, no other experimental data of the Born effective charge tensors for GaN and AlN exist.

The calculated Born effective charges $Z_{//}^*$ and Z_{\perp}^* decrease with increasing pressure. The pressure-induced reduction of the dynamical ion charges indicates a charge redistribution from the nitrogen atoms to the gallium or aluminum atoms in comparison with the pressure-free situation.

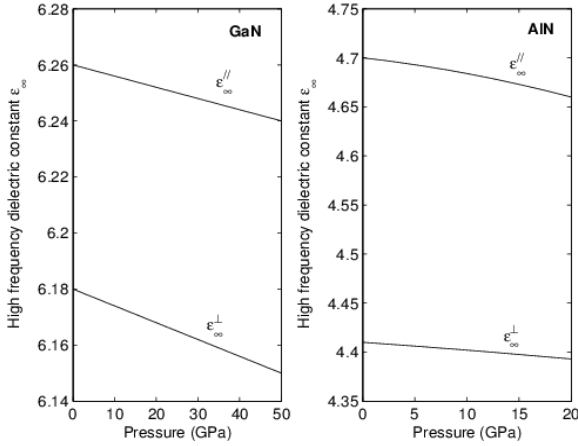


Fig. 5. High-frequency dielectric constant versus pressure for wurtzite GaN and AlN

Our results concerning $\epsilon_{\infty}^{\perp}$ and $\epsilon_{\infty}^{//}$ at zero pressure for GaN are found to be 6.18 and 6.26, and for AlN 4.41 and 4.70 respectively. Comparing our calculated data with those computed by the orthogonalized linear combination of atomic orbitals (OLCAO) (Refs. 25), and Pseudopotential calculations [26, 21], the agreement is good. However, Our values are bigger than those through full-potential linear-muffin-tin-orbital (LMTO) method [27]. The authors in Ref. 27 neglect the influence of local-field effects on the dielectric tensor, which, as reported, reduces the value of the dielectric constants by about 10–15% [28].

The average value $\epsilon(\infty) = (1/3)Tr\epsilon_{\infty}$ have also been calculated and found to be 4.5 for AlN and 6.2 for wurtzite GaN. These values agree to within 10% with the experimental some obtained by infrared reflectivity [29] and Raman-scattering [23]. However, one should note that the experimental data available for the stable structures of GaN and AlN are scarce and may suffer from the relatively low quality of the crystal samples. In addition,

the screening tends to overestimate average dielectric tensor in theoretical calculations performed within the LDA approximation.

The pressure dependence of $\epsilon_{\infty}^{\perp}$ and $\epsilon_{\infty}^{//}$ for GaN and AlN is shown in Fig. 4 and Fig. 5. Note that as pressure rises, $\epsilon_{\infty}^{\perp}$ and $\epsilon_{\infty}^{//}$ decrease monotonically, which is similar to what has been found for the most tetrahedrally coordinated semiconductors. Similar to that mode Grüneisen parameter, one can define a dielectric Grüneisen parameter

$$\gamma^{\epsilon} = -\frac{d \ln \epsilon}{d \ln V}, \quad (8)$$

to characterize the pressure dependence of the dielectric constants. For GaN and AlN, we have found that the perpendicular and parallel components of γ^{ϵ} are both negative with $\gamma^{\epsilon_{\infty}^{//}} = -0.397$, $\gamma^{\epsilon_{\infty}^{\perp}} = -0.381$ for GaN, and $\gamma^{\epsilon_{\infty}^{//}} = -0.582$, $\gamma^{\epsilon_{\infty}^{\perp}} = -0.473$ for AlN.

4. Conclusions

In summary, First-principles calculations in the framework of the DFPT are carried out to study the pressure dependences of structure, phonon and dielectric properties for wurtzite GaN and AlN. Our results show that pressure dependence of the wurtzite parameters c/a are reasonably well, as measured by high pressure x-ray diffraction studies. The calculated pressure dependence of optical phonon frequencies, Born effective charges, dielectric constants is agreement with other theoretical data available. However, the calculated pressure coefficients of optical phonon frequencies are smaller than other experimental values, and pressure dependence of the LO–TO splittings in AlN between calculated and experimental data is contrary. The pressure dependence of Z_{\perp}^* , $Z_{//}^*$, $\epsilon_{\infty}^{\perp}$ and $\epsilon_{\infty}^{//}$ for wurtzite GaN and AlN is decrescent monotonically as pressure rises, which is

similar to most tetrahedrally coordinated semiconductors.

Acknowledgements

Project supported by Natural Science Foundation of Hunan Province (Grant No. 13JJ3121) and Aid program for Science and Technology Innovative Research Team in Higher Educational Institutions of Hunan Province

References

- [1] E. F. Schubert and J. K. Kim, *Science* **308**, 1274 (2005).
- [2] T. Kuykendall, P. Ulrich, S. Aloni, P. Yang, *Nature Mater.* **6**, 951 (2007).
- [3] J. Simon, V. Protasenko, C. Lian, H. Xing, D. Jena, *Science* **327**, 60 (2010).
- [4] L. Dong, S. K. Yadav, R. Ramprasad, S. P. Alpay, *Appl. Phys. Lett.* **96**, 202106 (2010).
- [5] S. M. de Sousa Pereira, K. P. O'Donnell, E. J. da Costa Alves, *Adv. Funct. Mater.* **17**, 37 (2007).
- [6] P. Perlin, A. Polian, and T. Suski, *Phys. Rev. B* **47**, 2874 (1993).
- [7] M. Kuball, J. M. Hayes, A. D. Prins et al., *Appl. Phys. Lett.* **78**, 724 (2001).
- [8] A. R. Goñi, H. Siegle, K. Syassen, C. Thomsen, J. M. Wagner, *Phys. Rev. B* **64**, 035205 (2001).
- [9] E. V. Yakovenko, M. Gauthier, and A. Polian, *JETP* **98**, 981 (2004).
- [10] F. J. Manjón, D. Errandonea, A. H. Romero, N. Garro, J. Serrano, M. Kuball, *Phys. Rev. B* **77**, 205204 (2008).
- [11] P. Perlin, T. Suski, J. W. Ager, *Phys. Rev. B* **60**, 1480 (1999).
- [12] P. E. Van Camp, V. E. Van Doren, J. T. Devreese, *Solid State Commun.* **81**, 23 (1992). [13] M. Ueno, M. Yoshida, A. Onodera, O. Shimomura, K. Takemura, *Phys. Rev. B* **49**, 14 (1994).
- [14] M. Ueno, A. Onodera, O. Shimomura, K. Takemura, *Phys. Rev. B* **45**, 10 123 (1992).
- [15] S. Uehara, T. Masamoto, A. Onodera, M. Ueno, O. Shimomura, K. Takemura, *J. Phys. Chem. Solids* **58**, 2093 (1997).
- [16] X. Gonze, C. Lee, *Phys. Rev. B* **55**, 10 355 (1997).
- [17] Gonze X, Beuken J M, Caracas R, et al., *Comput. Mater. Sci.* **25**, 478 (2002).
- [18] M.C. Payne, M.P. Teter, D.C. Allan, T.A. Arias, J.D. Jonannopoulos, *Rev. Mod. Phys.* **64**, 1045 (1992).
- [19] N. Troullier, J.L. Martins, *Phys. Rev. B* **43**, 1993 (1991).
- [20] F. J. Manjón, D. Errandonea, N. Garro, A. H. Romero, J. Serrano, and M. Kuball, *phys. stat. sol. (b)* **244**, 42 (2007).
- [21] J. M. Wagner and F. Bechstedt, *Phys. Rev. B* **66**, 115202 (2002).
- [22] G. Venkataraman, L. A. Feldkamp, V. C. Sahni, *Dynamics of Perfect Crystals* (MIT Press, Cambridge, Massachusetts, 1975), P. 202.
- [23] J. A. Sanjurjo, E. Lopez-Cruz, P. Vogl, M. Cardona, *Phys. Rev. B* **28**, 5479 (1983).
- [24] J. Misek, F. Srobar, *Elektrotech. Cas.* **30**, 690 (1979).
- [25] Y. N. Xu, W. Y. Ching, *Phys. Rev. B* **48**, 4335 (1993).
- [26] Claudia Bungaro, Krzysztof Rapcewicz, J. Bernholc, *Phys. Rev. B* **61**, 6720 (2000).
- [27] N. E. Christensen, I. Gorczyca, *Phys. Rev. B* **50**, 4397 (1994).
- [28] K. Karch, F. Bechstedt, *Phys. Rev. B* **56**, 7404 (1997).
- [29] I. Gorczyca, N.E. Christensen, E.L. Pelzer y Blancá, C.O. Rodriguez, *Phys. Rev. B* **51**, 11 936 (1995).

*Corresponding author: whycs@163.com